JPET Fast Forward. Published on January 13, 2004 as DOI: 10.1124/jpet.103.061655

THE NEUROPROTECTIVE EFFECT OF TC-1698, A NOVEL ALPHA7 LIGAND, IS PREVENTED THROUGH ANGIOTENSIN II ACTIVATION OF A TYROSINE PHOSPHATASE

Mario B. Marrero, Roger L. Papke, Balwinder S. Bhatti, Seán Shaw,

and Merouane Bencherif

Vascular Biology Center (*M.B.M.*, *S.S.*), Department of Pharmacology and Toxicology (*M.B.M.*), Medical College of Georgia, Augusta, Georgia, Department of Physiology and Pharmacology, University of Florida, Gainesville (*R.L.P.*) Department Preclinical Research (*M.B.*) and Discovery and Development (*B.S.B.*), *Targacept Inc.,* Winston-Salem North-Carolina.

JPET Fast Forward. Published on January 13, 2004 as DOI: 10.1124/jpet.103.061655
This article has not been copyedited and formatted. The final version may differ from this version.

Running Title: Angiotensin II blocks TC-1698 Neuroprotection via SHP-1

Corresponding author: Merouane Bencherif MD, PhD; Vice President, Preclinical Research Targacept Inc.; 200 East First Street, Suite 300; Winston-Salem, NC 27101-4165; Tel: 336-480-2118; Fax: 336-480-2107; E-mail: merouane.bencherif@targacept.com

- √ 33 pages
- √ 1 Table
- √ 9 Figures
- √ 33 references
- √ Abstract: 236 words
- √ Introduction: 637 words
- √ Discussion: 879 words

List of Abbreviations: nAChR, nicotinic acetylcholine receptor; JAK2, Janus Kinase2; PI-3-K, phosphatydylinositol-3-kinase; PARP, poly-(ADP-ribose) polymerase; nAChR, nicotinic acetylcholine receptor; PTPase, protein tyrosine phosphatase; ACE, angiotensin converting enzyme; AD, Alzheimer's disease; Ang II, angiotensin II; PBS, phosphate-buffered saline; TBS,Tris-buffered saline; TTBS, Tris-Tween-20-buffered saline.

JPET Fast Forward. Published on January 13, 2004 as DOI: 10.1124/jpet.103.061655
This article has not been copyedited and formatted. The final version may differ from this version.

ABSTRACT

We have recently provided evidence for nicotine-induced complex formation between the alpha7 nAChR and the tyrosine-phosphorylated enzyme JAK2 that results in subsequent activation of PI-3-K and Akt. Nicotine interaction with the alpha7 nAChR inhibits Aβ (1-42) interaction with the same receptor, and the Aβ (1-42)-induced apoptosis is prevented through nicotine-induced activation of JAK2. These effects can be shown by measuring markers of cytotoxicity including the cleavage of the nuclear protein PARP, the induction of caspase 3, or cell viability.

In this study we found that TC-1698, a novel α7-selective agonist, exerts neuroprotective effects via activation of the JAK2/PI-3K cascade, which can be neutralized through activation of the Ang II AT_2 receptor. Vanadate not only augmented the TC-1698-induced tyrosine phosphorylation of JAK2 but also blocked the Ang II neutralization of TC-1698-induced neuroprotection against Aβ (1-42) induced cleavage of PARP. Furthermore, when SHP-1 was neutralized via antisense transfection, the Ang II inhibition of TC-1698-induced neuroprotection against Aβ (1-42) was prevented. These results support the main hypothesis which states that JAK2 plays a central role in the nicotinic α7 receptor-induced activation of the JAK2-PI-3K cascade in PC12 cells, which ultimately contribute to nAChR-mediated neuroprotection. Ang II inhibits this pathway through the AT_2 receptor activation of the Protein Tyrosine Phosphatase (PTPase) SHP-1. This study supports central and opposite roles for JAK2 and SHP-1 in the control of apoptosis and alpha7-mediated neuroprotection in PC12 cells.

JPET Fast Forward. Published on January 13, 2004 as DOI: 10.1124/jpet.103.061655
This article has not been copyedited and formatted. The final version may differ from this version.

Neuronal nicotinic acetylcholine receptors (nAChRs) are composed of various combinations of α-subunits (α2-α10) and β-subunits (β2-β4) that form homo- or heteropentamers. The alpha7 nAChR forms functional homomeric ligand-gated ion channels that promote rapidly desensitizing Ca^{2+} influx, is widely expressed throughout the mammalian brain, and has been implicated in sensory gating, cognition, inflammation and neuroprotection (Kem et al., 2000; Bencherif and Schmitt, 2002; Kitagawa et al., 2003; Wang et al., 2003;). The cholinergic deficit in neurodegenerative diseases has been clearly established and is the basis for current therapeutic strategies. There is an early and significant depletion of high affinity nicotinic receptors in the brains of Alzheimer's patient's (Breese et al., 1997; Court et al., 2001), with a selective loss of nAChR predominating in brain regions with β-amyloid deposition. A number of studies have shown cognitive improvement in rodents, and primates including humans following administration of ligands targeting nicotinic acetylcholine receptors (Newhouse et al., 2001). In addition to their known symptomatic effects, neuronal nicotinic ligands have shown neuroprotective activity *in vitro* and *in vivo* suggesting an additional potential for disease modification (Donnely-Roberts et al., 1996; Kihara et al., 2001; Nordberg et al., 2002). A direct interaction of the β-amyloid peptide with the alpha7 nAChR is suggested by recent findings. β-amyloid peptide interacts with high affinity to the alpha7 nAChR and results in functional non-competitive blockade in hippocampal neurons (Wang et al., 2000; Liu et al., 2001). In addition, nicotinic-induced neuroprotection against β-amyloid induced toxicity is suppressed by α-bungarotoxin (Bgt), and selective alpha7 nAChR agonists exert cytoprotective effects (Kem, 2000; Shaw et al, 2002).

Recent studies have reported that alpha7-mediated effects are mediated through phosphorylation of specific kinases such as Akt and subsequent activation of

JPET Fast Forward. Published on January 13, 2004 as DOI: 10.1124/jpet.103.061655
This article has not been copyedited and formatted. The final version may differ from this version.

phosphatidylinositol 3-kinase (Kihara et al., 2001). Another study has shown that while nicotine activates the PI-3-K neuroprotective cascade, Aβ (1-42) chronically activates the mitogen-activated protein kinase (MAPK) cascade via the hippocampal alpha7 nAChR (Dineley et al., 2001). These findings were interpreted as evidence that chronic activation of the MAPK pathway by Aβ (1-42) eventually leads to the down regulation of MAPK which then sets up a positive feedback for Aβ accumulation and decreased phosphorylation of the cAMP-regulatory protein (CREB) which is a necessary component for hippocampus-dependent memory formation in mammals. Nonetheless, these findings suggest that the alpha7 nAChR transduces signals to PI-3-K in a cascade, which ultimately contributes to a neuroprotective effect against Aβ (1-42).

There is recent evidence for the nicotine-induced complex formation between the alpha7 nAChR and the tyrosine-phosphorylated enzyme JAK2 that results in subsequent activation of PI-3-K, and Akt (Shaw et al., 2002). In addition, nicotine interaction with the alpha7 nAChR is "dominant" over Aβ (1-42) interaction with the receptor, and the Aβ (1-42)-induced apoptosis is prevented through the nicotine-induced activation of JAK2. These effects can be shown by measuring markers of cytotoxicity such as the cleavage of the nuclear protein PARP, the induction of caspase 3, or cell viability. Finally, we reported that neuroprotective effects of nicotine could be neutralized through activation of the angiotensin II AT_2 receptor as evidenced by the reversal of JAK2 phosphorylation and inhibition of nicotine-induced neuroprotection (Shaw et al., 2002).

In this study we report that TC-1698 is a highly selective nicotinic α7 receptor agonist, that it activates JAK2 in PC12 cells, and that this activation and downstream activation of PI-3-K and Akt are blocked by the specific inhibitor AG490. TC-1698-induced phosphorylation of JAK2 can be neutralized through angiotensin II (Ang II)-activation of the AT2 receptor and these

effects are mediated through the Protein Tyrosine Phosphatase (PTPase) SHP-1. Further, usage of the PTPase SHP-1 antisense identified central and opposite roles for Jak2 and SHP-1 in the control of alpha7 nAChR-mediated PC12 cell survival and apoptosis.

JPET Fast Forward. Published on January 13, 2004 as DOI: 10.1124/jpet.103.061655
This article has not been copyedited and formatted. The final version may differ from this version.

MATERIALS AND METHODS

Synthetic Procedures - The compound 2-(3-pyridyl)-1-azabicyclo[3.2.2]nonane (TC-1698) was prepared by the alkylation of the imine derived from 3-acetylpyridine and isopropylamine. Thus the sequential treatment of imine with LDA and 4-(bromomethyl)oxane provided the key intermediate 1-(3-pyridyl)-2-(4-oxanyl)propan-1-one, which was readily elaborated into the higher homologue of 2-(3-pyridyl)-quinuclidines. The construction of the [3.2.2] ring was accomplished by the transformation of the intermediate into oxime(1-pyridin-3-yl-3-(tetrahydropyran-4-yl)-propan-1-one oxime) and then to the amine(1-pyridin-3-yl-3-(tetrahydro-pyran-4-yl)-propylamine). The amine upon heating with concentrated HBr in a sealed tube, followed by removal of the acid and then refluxing with dilute ethanolic potassium carbonate yielded TC-1698 (see Fig. 1). The structure was confirmed by ^{1}H an ^{13}C NMR, GCMS and elemental analysis as 2-(3-pyridyl)-1-azabicyclo[3.2.2]nonane dihydrochloride (TC-1698) as 99.9% pure.

Binding studies.

Tissue preparation. Rats will be killed by decapitation after anesthesia with 70% CO_2. The brain will be rapidly removed and placed on an ice-cold platform. The cerebral cortex, cerebellum, hippocampus and striatum regions will be dissected and stored at –20^{o}C until used for membrane preparation.

Preparation of membranes from rat tissues. Tissue will be homogenized in 10 vol (w/v) of ice-cold preparative buffer (in mM: KCl, 11; KH_2PO_4, 6; NaCl, 137; Na_2HPO_4, 8; HEPES, 20; iodoacetamide, 5; EDTA, 1.5; PMSF, 0.1, pH 7.4 using a Polytron (Brinkmann Instruments, Westbury, NY) at setting 6 for 15 sec. The homogenate will then be centrifuged at 40,000 g for 20 min at 4^{o}C, the pellet resuspended in 20 vol of ice-cold water and incubated for 20 min at

JPET Fast Forward. Published on January 13, 2004 as DOI: 10.1124/jpet.103.061655
This article has not been copyedited and formatted. The final version may differ from this version.

4°C. The final pellet (40,000 g for 20 min at 4°C) will then be resuspended in preparative buffer and stored at -20°C. On the day of assay, tissue will be thawed, centrifuged at 40,000 g for 20 min at 4°C, then resuspended in Dulbecco's phosphate-buffered saline (PBS, # 21300, Invitrogen Corporation, Carlsbad, CA), pH. 7.4, to a final concentration of 2-3 mg/mL total protein. PBS with 0.05% BSA will be used to resuspend hippocampal membranes. Protein concentration will be determined by the Bradford method using BSA as the standard.

[^{3}H]-MLA and [^{3}H]-NIC binding assays. The [^{3}H]-MLA binding assay will be used to detect and quantify the α7 nAChRs in cerebral cortex, cerebellum, hippocampus and striatum as previously described (Davies et al., 1999). Briefly, each sample (150 µL of total volume) will consist of membrane suspension (~ 150 µg of protein), 5 nM [^{3}H]-MLA for single-point screening or 0.5–20 nM for the saturation analysis. Non-specific binding will be determined in the presence of 10 µM cold MLA. Binding reactions will be conducted for 2 h at RT in 96-well micro-titer plates in triplicate. The binding reaction is terminated by rapid filtration onto Whatman GF/B glass fiber filters, presoaked in 0.3% polyethyleneimine, using a tissue harvester (Brandel, Gaithersburg MD). After washing 5 times with ~ 350 µl of the ice-cold PBS, the filter plate will be dried at 49°C for approx. 2 h. MeltiLex A melt-on scintillator sheets (PerkinElmer) will then be applied to the dry filters and radioactivity bound to the membranes is determined by liquid scintillation counting. The[^{3}H]-NIC binding assay will use the same procedure to detect and quantify α4β2 nAChRs (Romano and Goldstein, 1980).

Preparation of RNA. - The human nAChR clones were obtained from Dr. Jon Lindstrom (University of Pennsylvania) and the mouse muscle subunit clones from Dr. Jim Boulter (UCLA); the mouse epsilon clone was provided by Dr. Paul Gardener. After linearization and

JPET Fast Forward. Published on January 13, 2004 as DOI: 10.1124/jpet.103.061655
This article has not been copyedited and formatted. The final version may differ from this version.

purification of cloned cDNAs, RNA transcripts were prepared *in vitro* using the appropriate mMessage mMachine kit from Ambion Inc. (Austin, TX).

Expression in Xenopus oocytes. - Mature (>9 cm) female Xenopus laevis African toads (Nasco, Ft. Atkinson, WI) were used as a source of oocytes. Prior to surgery, frogs were anesthetized by placing the animal in a 1.5 g/L solution of MS222 (3-aminobenzoic acid ethyl ester) for 30 min. Oocytes were removed from an incision made in the abdomen. In order to remove the follicular cell layer, harvested oocytes were treated with 1.25 mg/mL collagenase from Worthington Biochemical Corporation (Freehold, NJ) for 2 hours at room temperature in calcium-free Barth's solution (88 mM NaCl, 10 mM HEPES pH 7.6, 0.33 mM MgS04, 0.1 mg/mL gentamicin sulfate). Subsequently, stage 5 oocytes were isolated and injected with 50 nl (5-20 ng) each of the appropriate subunit cRNAs. Recordings were made 1 to 15 days after injection.

Electrophysiology. - Experiments were conducted using a beta version of OpusXpress 6000A (Axon Instruments, Union City California). OpusXpress is an integrated system that provides automated impalement and voltage clamp of up to eight oocytes in parallel. The beta unit used for these studies recorded from four cells simultaneously. Cells were automatically perfused with bath solution, and agonist solutions were delivered from a 96-well plate. Both the voltage and current electrodes were filled with 3 M KCl. The agonist solutions were applied via disposable tips, which eliminated any possibility of cross-contamination. Drug applications alternated between ACh controls and experimental applications. Flow rates were set at 1 mL/min. Cells were voltage-clamped at a holding potential of -60mV. Data were collected at 50Hz and filtered at 20 Hz. Drug applications were 20 seconds in duration followed by 383 second washout periods for $\alpha 7$ receptors and 10 seconds with 383 second wash periods for other subtypes.

JPET Fast Forward. Published on January 13, 2004 as DOI: 10.1124/jpet.103.061655
This article has not been copyedited and formatted. The final version may differ from this version.

Experimental protocols and data analysis. - Each oocyte received two initial control applications of ACh, then an experimental drug application, and then a follow-up control application of 300 μM ACh. The control ACh concentrations for α1β1εδ, α3β4, α4β2, α3β2, and α7 receptors were 30 μM, 100 μM, 10 μM, 30 μM, and 300 μM, respectively. These concentrations were determined to be the EC_{74}, EC_{15}, EC_{22}, EC_{18}, and EC_{100}, respectively. Responses to TC-1698 applications were calculated relative to the preceding ACh control responses in order to normalize the data, compensating for the varying levels of channel expression among the oocytes. Drug responses were initially normalized to the ACh control response values and then adjusted to reflect the TC-1698 responses relative to the ACh maximums. Responses for α7 receptors were calculated as net charge over a 90 s interval, beginning with the drug application (Papke and Papke 2002). For subtypes other than α7, responses were calculated from the peak current amplitudes. Means and standard errors (SEM) were calculated from the normalized responses of at least three oocytes for each experimental concentration. The application of some experimental drugs caused the subsequent ACh control responses to be reduced, suggesting some form of residual inhibition (or prolonged desensitization). In order to measure the residual inhibitory effects, this subsequent control response was compared to the pre-application control ACh response.

For concentration-response relations, data derived from net charge analyses were plotted using Kaleidagraph 3.0.2 (Abelbeck Software; Reading, PA), and curves were generated from the Hill equation

JPET Fast Forward. Published on January 13, 2004 as DOI: 10.1124/jpet.103.061655
This article has not been copyedited and formatted. The final version may differ from this version.

$$\text{Response} = \frac{I_{\max}[agonist]^n}{[agonist]^n + (EC50)^n}$$

where I_{max} denotes the maximal response for a particular agonist/subunit combination, and n represents the Hill coefficient. I_{max}, n, and the EC_{50} were all unconstrained for the fitting procedures. Negative Hill slopes were applied for the calculation of IC_{50} values.

Materials and Chemicals. - Chemicals for electrophysiology were obtained from Sigma Chemical Co. (St. Louis, MO) with the exception of TC-1698 which was synthesized. Other chemicals were purchased from Aldrich Chemical Company (Milwaukee, Wisconsin). These were used without further purification, except in the case of THF, which was dried by distillation from sodium and benzophenone. Merck silica gel 60 (70-230 mesh) was used for all the chromatographic purifications. Molecular weight standards, acrylamide, sodium dodecyl sulfate (SDS), N-N'-methylene-bisacrylamide, N,N,N',N'-tetramethylenediamine, protein assay reagents and nitrocellulose membranes were purchased from Bio-Rad Laboratories (Hercules, CA, USA). Protein A/G-agarose was obtained from Santa-Cruz Biotechnology (Santa Cruz, CA, USA) whereas Dulbecco's modified Eagle's medium (DMEM; GIBCO/BRL, Gaithersburg, MD)), fetal bovine serum (Atlanta Biologicals, Norcross, GA), trypsin, and all medium additives were obtained from Mediatech Inc. (Herndon, VA, USA). Monoclonal antibody to phosphotyrosine (PY20) and SHP-2 were procured from Transduction Laboratories (Lexington, KY, USA). PARP antibodies were purchased from New England Biolabs (Beverly, MA, USA). Anti-phosphotyrosine JAK2 and JAK2 antibodies were obtained from Biosource International (Camarillo, CA, USA). The Pierce Supersignal substrate chemiluminescence detection kit was obtained from Pierce (Rockford, IL, USA). Goat anti-mouse IgG and anti-rabbit IgG were acquired from Amersham (Princeton, NJ, USA), and tween-20, Aβ (1-42) peptide, anti-Aβ (1-

JPET Fast Forward. Published on January 13, 2004 as DOI: 10.1124/jpet.103.061655
This article has not been copyedited and formatted. The final version may differ from this version.

42) and anti-α7 nAChR and all other chemicals were purchased from Sigma Chemical Corp. (St. Louis, MO, USA).

Isolation and Culture of PC12 cells - PC12, rat pheochromocytoma cells, were maintained in proliferative growth phase in DMEM supplemented with 10% horse serum, 5% fetal calf serum and antibiotics (penicillin/streptomycin) according to routine protocols (Bencherif et al., 1996).

Western blotting studies of JAK2 - The tyrosine phosphorylation of JAK2 was determined in serum-starved PC12 cells stimulated with 10 μM TC-1698 (0 min to 60 min) in the presence or absence of 10 μM (1 hour pre-incubation) of the JAK2 specific inhibitor AG-490 (Meydan et al., 1996; Dicou et al., 2001). While many tyrosine kinase inhibitors are often promiscuous in the enzyme they target, AG-490 is unique in that it does not inhibit other tyrosine kinases such as Lck, Lyn, Btk, Syk, Src, JAK1, or Tyk2 (Meydan et al., 1996). At the end of stimulation, cells were washed twice with ice-cold PBSV (phosphate-buffered saline with 1 mmol/L Na_3VO_4). Each dish was then treated for 60 min with ice-cold lysis buffer (20 mmol/L Tris-HCl, pH 7.4, 2.5 mmol/L EDTA, 1% Triton X-100, 10% glycerol, 10 mmol/L $Na_4P_2O_7$, 50 mmol/L NaF, 1 mmol/L Na_3VO_4 and 1 mmol/L PMSF), and the supernatant fraction was obtained as cell lysate by centrifugation at 58 000*g* for 25 min at 4ºC. Samples were resolved by 10% SDS-PAGE gel electrophoresis, transferred to a nitrocellulose membrane and blocked by 60-min incubation at 22 ºC in TTBS (TBS with 0.05% Tween-20, pH 7.4) plus 5% skimmed milk powder. The nitrocellulose membrane was incubated overnight at 4ºC with affinity-purified anti-phospho specific JAK2 antibodies. The nitrocellulose membranes were washed 10 min twice with TTBS and incubated with goat anti-rabbit IgG horseradish peroxidase conjugate. After extensive washing, the bound antibody was visualized on a Kodak Biomax film using a Pierce Supersignal substrate chemiluminescence detection kit.

JPET Fast Forward. Published on January 13, 2004 as DOI: 10.1124/jpet.103.061655
This article has not been copyedited and formatted. The final version may differ from this version.

Immunoprecipitation studies of SHP-1 - The cell lysate prepared as described above is incubated with 10 µg/mL of anti-SHP-1 monoclonal antibodies at 4ºC for 2 hours and precipitated by addition of 50 µl of protein A/G agarose at 4ºC overnight. The immunoprecipitates is recovered by centrifugation and washed three times with ice-cold wash buffer (TBS, 0.1% Triton X-100, 1 mmol/L PMSF, and 1 mmol/L Na_3VO_4). Immunoprecipitated proteins are dissolved in 100 µl of LaemmLi sample buffer and 80 µl of each sample resolved by SDS-PAGE gel electrophoresis. Samples are transferred to a nitrocellulose membrane and blocked by 60-min incubation at room temperature (22ºC) in TTBS plus 5% skimmed milk powder. The nitrocellulose membrane is then incubated overnight at 4ºC with 10 µg/mL of affinity-purified anti-phosphotyrosine antibodies. The nitrocellulose membranes were washed for 10 min twice with TTBS and incubated with goat anti-mouse IgG horseradish peroxidase conjugate. After extensive washing, the bound antibody was visualized on a Kodak Biomax film using a Pierce Supersignal substrate chemiluminescence detection kit.

SHP-1 tyrosine phosphatase activity assay. - SHP-1 activity was determined as previously described (Marrero et al., 1998). Briefly, SHP-1 proteins were immunoprecipitated with anti-SHP-1 antibodies from PC12 cell lysates and the immunocomplexes were washed three times with ice-cold wash buffer and then three times with phosphatase buffer (50 mM HEPES, 60 mM NaCl, 60 mM KCl, 0.1 mM PMSF, 10 µg/mL aprotinin, and 10 µg/mL leupeptin, pH 7.4). Phosphatase activity was measured by monitoring the rate of formation of *p*-nitrophenol by dephosphorylation of *p*-nitrophenyl phosphate. Immunocomplex pellets were thus resuspended in 100 µl of phosphatase buffer containing 1 mg/mL BSA, 5 mM EDTA, and 10 mM dithiothreitol. The reaction was initiated by the addition of *p*-nitrophenyl phosphate (10 mM final concentration). After a 30-min incubation at room temperature, the reaction was stopped by the

JPET Fast Forward. Published on January 13, 2004 as DOI: 10.1124/jpet.103.061655
This article has not been copyedited and formatted. The final version may differ from this version.

addition of 1 M NaOH and absorbance of the sample was determined at 410 nm in a spectrophotometer.

Antisense against SHP-1- An antisense oligonucleotide that targets the translational start site of the murine SHP-1 coding sequence (5′-ACCTCACCATCCTTGGGGT-3′) has been found to significantly reduce SHP-1 expression in human erythroleukemic SKT6 cells (Sharlow et al., 1997). Therefore, we have tested the effect of SHP-1 antisense phophorothiorate oligonucleotide on SHP-1 expression in PC12 cells. Cells were treated with the sense, or antisense oligonucleotides (10 μM) in lipofectamine for various times, SHP-1 was immunoprecipitated, and the immunoprecipitates were immunoblotted with anti-SHP-1 antibody.

Assessment of PC12 cell apoptosis - Apoptosis is determined by assessing the cleavage of the DNA-repairing enzyme PARP using a western blot assay. PARP (116-kDa) is an endogenous substrate for caspase-3, which is cleaved to a typical 85-kDa fragment during various forms of apoptosis. PC12 cells are treated with 0.1 μM Aβ for 8 hours in the presence or absence of TC-1698 and/or AG-490. The cells are collected, washed with PBS, and lysed in 1 mL of SDS-PAGE sample buffer boiled for 10 min. Total cell lysates (30 μg of protein) are separated by SDS-PAGE and transferred to nitrocellulose membranes. The membranes are blocked for 1 h at 25°C with 5% nonfat dry milk in TBST (25 mM Tris-HCl, pH 7.5, 0.5 M NaCl, 0.05% Tween-20). Membranes are incubated with primary PARP antibody specific for the 85-kDa fragments for 2-3 h at 25°C, rinsed with TBST, and incubated with secondary antibody for 1 h at 25°C. Immunodetection is performed with appropriate antibody using an enhanced chemiluminescence (ECL) system (Amersham).

Caspase 3 enzyme activity is determined with a fluorogenic substrate for caspase-3 in crude PC12 cell extracts. The caspase 3 fluorogenic peptide Ac-DEVD-AMC (Promega,

JPET Fast Forward. Published on January 13, 2004 as DOI: 10.1124/jpet.103.061655
This article has not been copyedited and formatted. The final version may differ from this version.

Madison, WI) contains the specific caspase 3 cleavage sequence (DEVD) coupled at the C-terminal to the fluorochrome 7-amino-4-methyl coumarin. The substrate emits a blue fluorescence when excited at a wavelength of 360 nm. When cleaved from the peptide by the caspase 3 enzyme activity in the cell lysate, free 7-amino-4-methyl coumarin is released and can be detected by its yellow/green emission at 460 nm. Appropriate controls included a reversible aldehyde inhibitor of caspase 3 to assess the specific contribution of the caspase 3 enzyme activity (data not shown). Fluorescence units were normalized relative to total protein concentration of the cell extract. We performed the assays in triplicate and repeated the experiments six times.

Data analysis - All statistical comparisons were made using Student's *t* test for paired data and analysis of variance (ANOVA). Significance was $p < 0.05$.

JPET Fast Forward. Published on January 13, 2004 as DOI: 10.1124/jpet.103.061655
This article has not been copyedited and formatted. The final version may differ from this version.

RESULTS

Electrophysiological studies indicate that TC-1698 is a selective agonist to the alpha7 nAChR.

α4β2 nAChR. TC-1698 had little or no agonist activity when applied alone at concentrations up to 100 μM to oocytes expressing α4β2 receptors (<3% ACh maximum, Figure 2). However, subsequent to the application of TC-1698, we noted that subsequent ACh control responses were progressively inhibited (IC_{50} > 30 μM, Figure 3). Since we noted an inhibition of α4β2 control ACh responses following the application of TC-1698, we further investigated whether TC-1698 might function as an antagonist of α4β2 nAChR. When TC-1698 was co-applied at increasing concentration with 30 μM ACh, we noted a concentration-dependent inhibition of the ACh response (IC_{50} ≈ 300 nM, Figure 3). In order to further investigate the nature of the TC-1698 inhibition of α4β2 ACh responses, we conducted some competition experiments. We noted that when TC-1698 at a fixed concentration of 1μM was co-applied with increasing concentrations of ACh, there was inhibition of the response to low concentrations of ACh but not to high concentrations of ACh, consistent with competitive inhibition (Figure 3; Table II).

α3β2 *nAChR* . TC-1698 also had relatively little activity when applied alone at concentrations up to 300 μM to oocytes expressing α3β2 receptors (<5% ACh maximum, Figure 2; Table II). However, subsequent ACh responses were decreased after TC-1698 was applied alone (IC_{50} ≈ 25 μM, not shown).

α3β4 *nAChR* . When TC-1698 was applied to oocytes expressing α3β4 receptors, very small currents were observed at very high concentrations (Imax ≈5% that of ACh, EC_{50} =1600

JPET Fast Forward. Published on January 13, 2004 as DOI: 10.1124/jpet.103.061655
This article has not been copyedited and formatted. The final version may differ from this version.

μM, Figure 2). After the application of TC-1698 to oocytes expressing α3β4 receptors, little or no inhibition of subsequent ACh control responses was observed (data not shown).

α1β1εδ *nAChR* . TC-1698 was also a relatively potent and modestly efficacious agonist of mouse muscle nAChR expressed in *Xenopus* oocytes. The maximum current was 28 ±1% of the maximum response to ACh. TC-1698 had an EC_{50} of 20 ±1.3 μM, fifty times less potent than for α7, compared to 82 μM for ACh (Figure 2).

α7 *nAChR* . While TC-1698 had very little agonist activity with beta subunit-containing neuronal nAChR, it appeared to be a potent and efficacious agonist of α7-type receptors. It produced maximum responses equivalent to those produced by ACh (i. e. Imax ≥ 100% compared to ACh). TC-1698 was approximately 30-fold more potent than ACh, with an EC_{50} of 440 ± 14 nM, compared to 30 μM for ACh (Figure 2). TC-1698 application to α7-expressing oocytes produced no significant residual inhibition of subsequent ACh responses (data not shown). In Figure 2a, note that because TC-1698 is a far more potent agonist than ACh, although the TC-1698 peak current is larger than that of the ACh controls, the net charge is roughly equivalent to that evoked by the 300 μm ACh control.

Activity profile for TC1698 in clonal cells

The affinity of TC-1698 for brain nAChR was determined by radioligand binding studies. Membranes prepared from rat hippocampus, a brain region enriched in α7 nAChR, were used along with [^{3}H]-methyllycaconitine [MLA] as labeling agent and TC-1698 exhibited a Ki of 11 ± 1.7 nM in this preparation (n = 4). The potency and efficacy of TC-1698 at peripheral nAChR was assessed using radioactive rubidium efflux assays in rat and human cell lines expressing muscle- and ganglion-type nAChR (Lukas and Cullen, 1988). TC-1698 is a poor activator of rat and human ganglion-type nAChR and human muscle type receptors expressed in clonal cell

JPET Fast Forward. Published on January 13, 2004 as DOI: 10.1124/jpet.103.061655
This article has not been copyedited and formatted. The final version may differ from this version.

lines. At 100 μM activation of either human muscle receptor (human TE671/RD) or ganglion-type receptors (rat PC12 and human SH-SY5Y cells) were below 20% of that of nicotine. The intrinsic activity of TC-1698 at brain nAChR was assessed using [^{3}H]-dopamine ([^{3}H]-DA) release from rat striatal synaptosomes. TC-1698 resulted in no significant activation of dopamine release suggesting a lack of agonist activity at α4β2 nAChR (Bencherif et al., 2000).

A binding profile was conducted to evaluate the interaction of TC-1698 with other receptors, transporters, enzymes or ion channels. With the exception of nicotinic receptors at which binding was totally displaced, 10 μM TC-1698 had no or very low affinity for all binding sites examined (Table I).

Effects of the JAK2 inhibitor AG-490 on TC-1698-induced tyrosine phosphorylation of JAK2 and PI-3-Kinase and serine phosphorylation of Akt in PC12 cells.

Enzymatic activation of JAK2 is determine via its tyrosine phosphorylation. The tyrosine phosphorylated JAK2 sometimes shows up as a doublet or shifts in its migration in the SDS-PAGE gel. These anomalies may be due to either proteolysis of JAK2 or different levels of serine phosphorylation of the enzyme (Marrero et al, 1998 and Shaw et al, 2002). In this study we found that JAK2 is tyrosine phosphorylated in response to the α7 receptor specific ligand, TC-1698 (10 μM) within 5 minutes and this activation remained above basal levels even after longer exposure (60 minutes) to compound TC-1698 (Figure 4). We also found that preincubation for 1 hour with the JAK2 inhibitor AG-490 (10 μM) inhibited the TC-1698-induced JAK2 tyrosine phosphorylation, the tyrosine phosphorylation of PI-3-K and the serine phosphorylation of Akt (Figure 4). These results are similar in their kinetics of JAK2 activation to our previous reported results when we utilized nicotine (Shaw et al., 2002).

JPET Fast Forward. Published on January 13, 2004 as DOI: 10.1124/jpet.103.061655
This article has not been copyedited and formatted. The final version may differ from this version.

Effects of Ang II pretreatment with or without Ang II receptor antagonists on TC-1698-induced tyrosine phosphorylation of JAK2

Preincubation of PC12 cells with Ang II blocked TC-1698 induced tyrosine phosphorylation of JAK2 (Figure 5A). This inhibition was completely prevented by pre-incubation with an AT_2 antagonist (PD 123177 at 100 nM) but not by an AT_1 antagonist (candesartan at 100 nM) (Figure 5A) consistent with the Ang II receptor phenotype expressed in PC12 cells. Consistent with our data indicating that TC-1698 is a potent selective agonist of α7-type receptors, TC-1698-induced activation of JAK2 was blocked by the alpha 7 antagonist alpha bungoratoxin (Figure 5C).

Ang II-induced activation and tyrosine phosphorylation of SHP-1, and its effects on TC-1698-induced tyrosine phosphorylation of JAK2.

The AT_2 receptor exerts growth-inhibitory effects in cultured cells and *in vivo*, one of which has been proposed to be programmed cell death (Lehtonen et al., 1999; Horiuchi et al., 1998). Despite growing interest in AT_2 receptor-mediated apoptosis, relatively little is known about the molecular basis of this process. Recently growth-inhibitory effects of the AT_2 receptor have been reported to be mediated by the activation of PTPases, AT_2 receptor stimulation is associated with a rapid activation of SHP-1 in rat pheochromocytoma PC12 cells (Horiuchi et al., 1998). However, at present, no functional role has been demonstrated for SHP-1 activation by the AT_2 receptor, and it is interesting to note that SHP-1 has been shown to function as a negative regulator of JAK2 signaling (Marrero et al., 1998). Therefore, the potential biological significance of AT_2 receptor-induced programmed cell death led us to investigate whether SHP-1

JPET Fast Forward. Published on January 13, 2004 as DOI: 10.1124/jpet.103.061655
This article has not been copyedited and formatted. The final version may differ from this version.

activation could be involved in this process. We found that Ang II induced both the tyrosine phosphorylation and activation of SHP-1 (Figure 5B) and that vanadate, a specific inhibitor of PTPases (Marrero et al., 1996), blocked the activation of SHP-1 directly (Figure 6). Furthermore, vanadate also augmented TC-1698-induced tyrosine phosphorylation of JAK2 (Figure 6).

Antisense against SHP-1 and its effects on TC-1698-induced tyrosine phosphorylation of JAK2 in PC12 cells.

Since vanadate is not a specific inhibitor of SHP-1, we also tested the effect of SHP-1 antisense phophorothiorate oligonucleotide on SHP-1 expression in PC12 cells. Cells were treated with the sense, or antisense oligonucleotides (10 μM) for various times, SHP-1 was immunoprecipitated, and the immunoprecipitates immunoblotted with anti-SHP-1 antibody. As shown in Figure 7A, the antisense (but not the sense) oligonucleotide was effective in completely inhibiting SHP-1 expression within 12 hours. We then tested whether these antisense oligos could be used to regulate the TC-1698-induced activation JAK2 in PC12 cells. PC12 cells were stimulated with Ang II and lysed. JAK2 was then immunoprecipitated from lysates with anti-JAK2 antibody. Immunoprecipitated proteins were separated by gel electrophoresis, transferred to nitrocellulose, and then immunoblotted with anti-phosphotyrosine antibody. As a control, cells were exposed to SHP-1 sense oligonucleotide. As shown in Figure 7B, when cells were exposed to the SHP-1 antisense form 12 hours, JAK2 tyrosine phosphorylation was augmented. These results suggest that SHP-1 is the PTPase that dephosphorylates JAK2 following TC-1698-induced JAK2 phosphorylation in PC12 cells.

Assessment of PC12 cell apoptosis.

JPET Fast Forward. Published on January 13, 2004 as DOI: 10.1124/jpet.103.061655
This article has not been copyedited and formatted. The final version may differ from this version.

Apoptosis is determined by assessing the cleavage of the DNA-repairing enzyme PARP using a western blot assay. PC12 cells are treated with 0.1 μM Aβ for 8 hours in the presence or absence of TC-1698 (10 μM). As shown in Figure 8, PARP (116-kDa) was cleaved to its 85-kDa fragment following Aβ (1-42) treatment. The Aβ (1-42) induced cleavage of PARP was blocked by TC-1698, which was prevented by preincubation with AG-490 or Ang II (Figure 8). Further 12 h pre-treatment with SHP-1 antisense, but not sense, completely prevented the cleavage of PARP (compare lane 8 and 10). These results support our main hypothesis which states that JAK2 plays a central role in the nicotinic alpha 7 receptor-induced neuroprotection, which Ang II blocks through the AT_2 receptor activation of the PTPase SHP-1.

Apoptosis was also determined by activation of caspase 3. Caspase 3 is expressed in PC12 cells and is known to be involved in apoptosis (Shaw et al., 2002). Therefore, we examined caspase 3 activity following Ang II-induced apoptosis. We used the fluorescent peptide substrate Ac-DEVD-7AMC to measure caspase 3-like activity in cell lysates. As shown in Figure 9, the caspase 3-like activity that resulted in the cleavage of the peptide substrate Ac-DEVD-7AMC is evident after two hours of Ang II treatment and increased over time until it reached a peak after eight hours of treatment. However, the Ang II- induced activation of caspase 3 was blocked significantly in the presence of SHP-1 antisense ($+P < 0.01$) or vanadate ($*P < 0.01$) (Figure 9). Co-incubation with the SHP-1 sense had no effect on the Ang II- induced activation of caspase 3. In addition, incubation with TC-1698 had also no effect caspase 3 activation (Figure 9).

JPET Fast Forward. Published on January 13, 2004 as DOI: 10.1124/jpet.103.061655
This article has not been copyedited and formatted. The final version may differ from this version.

DISCUSSION

In this study we found that TC-1698, a novel α7-selective ligand, exerted neuroprotective effects via activation of the JAK2/PI-3K cascade, which can be neutralized through activation of the Ang II AT_2 receptor. The Ang II AT_2 receptor effects are reversed by nullifying a PTPase as evidenced by the usage of the PTPase specific inhibitor vanadate (Marrero et al., 1996). Vanadate not only augmented the TC-1698-induced tyrosine phosphorylation of JAK2 but also blocked the Ang II neutralization of TC-1698-induced neuroprotection against Aβ (1-42) induced cleavage of PARP. Furthermore, when we also neutralized SHP-1 via antisense transfection the Ang II neutralization of TC-1698-induced neuroprotection against Aβ (1-42) was again blocked. These results support our main hypothesis which states that JAK2 plays a central role in the nicotinic α7 receptor-induced activation of the JAK2-PI-3K cascade in PC12 cells, which ultimately contribute to nAChR-mediated neuroprotection. Furthermore, we also found that Ang II blocked this pathway through the AT_2 receptor activation of SHP-1.

TC-1698 was relatively potent as an antagonist of the ACh responses of α4β2 receptors, apparently working through a competitive mechanism. TC-1698 also blocked subsequent ACh control responses of α4β2 and α3β2 receptors after it was applied in the absence of ACh. Interestingly, TC-1698 appears to be a full potent agonist only for the α7 receptors. TC-1698 should predominantly activate α7 and inhibit α4β2 with relatively little effect on other receptors. TC-1698 appears to be a weak partial agonist/antagonist of beta subunit-containing neuronal receptors. The studies were conducted in PC12 cells with similar effects to those observed in human SH-SY5Y cells. Both of these cell lines exhibit α7 and α3β4-containing receptors and TC-1698 interacts with the former but not the later.

JPET Fast Forward. Published on January 13, 2004 as DOI: 10.1124/jpet.103.061655
This article has not been copyedited and formatted. The final version may differ from this version.

Several reports have documented the apoptotic effects of Ang II through AT_2 receptors. AT_2 receptors are expressed in PC12 and have been shown to inhibit the JAK/STAT signaling cascade (Kunioku et al., 2001). In contrast to nicotine-induced neuroprotection against β-Amyloid (1-42), pre-treatment of cells with Ang II blocks nicotine-induced activation of JAK2 via the AT_2 receptor and completely prevents nicotine mediated neuroprotective effects further suggesting a pivotal role for JAK2 phosphorylation (Shaw et al., 2002). Our findings in this study are consistent with the opposite roles on cell viability that exist between the alpha7 nAChR and the AT_2 receptor with activation of the AT_2 receptor overriding the potential benefit through the alpha7 nAChR. These results and the convergence of these pathways on phosphorylated JAK2 suggest that recruitment of nicotinic alpha7 nAChR receptor-mediated neuroprotection against Aβ (1-42) may be optimized under conditions where the AT_2-mediated inhibition is minimized by blocking the AT_2-induced activation of the PTPase SHP-1. Therefore, the findings in this study identify novel molecular mechanisms, which are fully consistent with the role attributed to alpha7 nAChR-induced activation of JAK2 and subsequent neuroprotective effect, AT_2-induced activation of SHP-1 and its purported role in apoptotic events.

SHP-1 is a soluble tyrosine phosphatase that participates in the negative regulation of the tyrosine kinase JAK2 (Marrero et al., 1998), and it has been recently reported that stimulation of AT_2 receptors rapidly activates SHP-1 in N1E-115 and AT_2-transfected Chinese hamster ovary (CHO) cells (Lehtonen et al., 1999; Horiuchi et al., 1998). In the present study, we document that the Ang II AT_2 receptor activates SHP-1 in PC12, and that the TC-1698 induced activation of JAK2 is augmented by SHP-1 antisense transfection. These results suggest that both SHP-1 activation and JAK2 deactivation constitute sequential events in the same signaling pathway.

JPET Fast Forward. Published on January 13, 2004 as DOI: 10.1124/jpet.103.061655
This article has not been copyedited and formatted. The final version may differ from this version.

Nicotinic neurotransmission is compromised in the brains of AD patients and accumulating evidence suggests that nAChR-selective ligands can offer neuroprotective effects in a number of *in vitro* models including neuronal death resulting from β-amyloid toxicity, NMDA-mediated cytotoxicity or growth factor deprivation and in *in vivo* models including chemically-induced neurotoxicity (MPTP models and systemic kainic acid-induced excitotoxic effects). Nicotinic ligands reduce β-amyloid aggregation and toxicity and inhibit amyloid deposition in transgenic mice with APPsw (Nordberg et al., 2002). A recent report has demonstrated that the alpha7 nAChR is also an essential regulator of inflammation and is required for inhibition of cytokine release (Wang et al., 2003). The physiological mechanism coined "the cholinergic anti-inflammatory pathway" which has been proposed to have major implications in immunology and therapeutics remains unknown. The induction and resolution of inflammatory processes are the complex outcome of interplay between pro- and anti-inflammatory cytokines. Pleiotropic cytokines such as IL-6 and IL-10 have been shown to activate the JAK-STAT pathway and act in opposition to effects mediated by the pro-inflammatory cytokines IL-1, TNF-α (Ahmed and Ivashkiv, 2000). It is conceivable from these findings that multifaceted therapeutic potential targeting cognitive deficits, neuroprotection, and inflammation in neurodegenerative diseases can be recruited through a single pharmacology targeting the alpha7 nAChR. It remains to be established whether similar pathways are operative for these various end-points *in vivo* and whether the negative influence of AT_2 stimulation is clinically relevant. However, the putative beneficial effects of ACE inhibitors in Alzheimer's disease and the observation of selective up-regulation of AT_2 receptor density (Ge and Barnes, 1996) and biosynthetic enzymes (Narain et al., 2000; Savaskan et al., 2001) concurrent with down-regulation of nAChR in the temporal cortex of some AD patients (Court et

al., 2001) is consistent with the opposite effects on cell viability observed in our studies through activation of AT_2 and alpha7-nAChR.

Acknowledgements: This work was supported by Targacept Inc. (to *MBM, RLP, SS*), and in part by NIH Grants HL58139 and DK50268 (*MBM*), the American Heart Association Established Investigator Award (*MBM*), and NIH grant PO1 AG10485 (to *RLP*). We thank Julia Porter Papke, Irena Garic, Bernadette Schoneburg and Clare Stokes for technical assistance. We are very grateful to Axon Instruments for the use of an OpusXpress 6000A and pClamp 9. We particularly thank Dr. Cathy Smith-Maxwell for her support and help with OpusXpress.

REFERENCES

Ahmed ST and Ivashkiv LB (2000) Inhibition of IL-6 and IL-10 signaling and Stat activation by inflammatory and stress pathways. *J Immunol* **165**: 5227-5237.

Barnes NM, Cheng CH, Costall B, Naylor RJ, Williams TJ and Wischik CM (1991) Angiotensin converting enzyme density is increased in temporal cortex from patients with Alzheimer's disease. *Eur J Pharmacol* **200**: 289-292.

Bencherif M, Lovette ME, Fowler KW, Arrington S, Reeves L, Caldwell WS and Lippiello PM (1996) RJR-2403: a nicotinic agonist with CNS selectivity I. In vitro characterization. *J Pharmacol Exp Ther* **279**: 1413-1421.

Bencherif M and Schmitt JD (2002) Targeting Neuronal Nicotinic Receptors: A Path To New Therapies. *CNS and Neurological Disorders*. **1**: 319-327

Breese CR, Adams C, Logel J, Drebing C, Rollins Y, Barnhart M, Sullivan B, Demasters BK, Freedman R and Leonard S (1997) Comparison of the regional expression of nicotinic acetylcholine receptor alpha7 mRNA and [125I]-alpha-bungarotoxin binding in human postmortem brain. *J Comp Neurol* **387**: 385-398.

Court J, Martin-Ruiz C, Piggott M, Spurden D, Griffiths M and Perry E (2001) Nicotinic receptor abnormalities in Alzheimer's disease. *Biol Psychiatry* **49**: 175-184.

Davies AR, Hardick, DJ, Blagbrough, IS, Potter, BV, Wolstenholme A.J, and Wonnacott S (1999). Characterization of the binding of [3H] methyllycaconitine: a new radioligand for labelling alpha 7-type neuronal nicotinic acetylcholine receptors. Neuropharmacology, *38*: 679-690.

Dicou E, Attoub S and Gressens P (2001) Neuroprotective effects of leptin in vivo and in vitro. *Neuroreport* **12**: 3947-3951.

Digicaylioglu M and Lipton SA (2001) Erythropoietin-mediated neuroprotection involves cross-talk between Jak2 and NF-kappaB signalling cascades. *Nature* **412**: 641-647.

Dineley KT, Westerman M, Bui D, Bell K, Ashe KH and Sweatt JD (2001) Beta-amyloid activates the mitogen-activated protein kinase cascade via hippocampal alpha7 nicotinic acetylcholine receptors: In vitro and in vivo mechanisms related to Alzheimer's disease. *J Neuroscience* **21**: 4125-4133.

Donnelly-Roberts DL, Xue IC, Arneric SP and Sullivan JP (1996) In vitro neuroprotective properties of the novel cholinergic channel activator (ChCA), ABT-418. *Brain Res* **719**: 36-44.

Ge J and Barnes NM (1996) Alterations in angiotensin AT1 and AT2 receptor subtype levels in brain regions from patients with neurodegenerative disorders. *Eur J Pharmacol* **297**: 299-306.

Horiuchi M, Akishita M and Dzau VJ (1998) Molecular and cellular mechanism of angiotensin II-mediated apoptosis. *Endocr Res* **24**: 307-314,

Kem WR (2000) The brain alpha7 nicotinic receptor may be an important therapeutic target for the treatment of Alzheimer's disease: studies with DMXBA (GTS-21). *Behav Brain Res* **113**: 169-181.

Kihara T, Shimohama S, Sawada H, Honda K, Nakamizo T, Shibasaki H, Kume T and Akaike A (2001) alpha 7 nicotinic receptor transduces signals to phosphatidylinositol 3- kinase to block A beta-amyloid-induced neurotoxicity. *J Biol Chem* **276**: 13541-13546.

Kitagawa H, Takenouchi T, Azuma R, Wesnes K. A, Kramer WG, Clody D. E and Burnett AL (2003) Safety, pharmacokinetics, and effects on cognitive function of multiple doses of GTS-21 in healthy, male volunteers. Neuropsychopharmacology 28: 542-51

Kunioku H, Inoue K and Tomida M (2001) Interleukin-6 protects rat PC12 cells from serum deprivation or chemotherapeutic agents through the phosphatidylinositol 3-kinase and STAT3 pathways. *Neurosci Lett* **309**: 13-16.

Lehtonen JY, Daviet L, Nahmias C, Horiuchi M and Dzau VJ (1999) Analysis of functional domains of angiotensin II type 2 receptor involved in apoptosis. *Mol Endocrinol* **13**: 1051-1060.

Liu Q, Kawai H and Berg DK (2001) beta -Amyloid peptide blocks the response of alpha 7-containing nicotinic receptors on hippocampal neurons. *Proc Natl Acad Sci U.S.A* **9**8: 4734-4739.

Lukas RJ and Cullen MJ (1988) An isotopic rubidium ion efflux assay for the functional characterization of nicotinic acetylcholine receptors in clonal cell lines. Anal. Biochem. 175: 212-218.

Marrero MB, Schieffer B, Bernstein KE and Ling BN (1996) Angiotensin II-induced tyrosine phosphorylation in mesangial and vascular smooth muscle cells. *Clin Exp Pharmacol Physiol* **23**: 83-88.

Marrero MB, Venema VJ, Ju H, Eaton DC and Venema RC (1998) Regulation of angiotensin II-induced JAK2 tyrosine phosphorylation: roles of SHP-1 and SHP-2. *Am J Physiol* **275**: C1216-C1223.

Meydan N, Grunberger T, Dadi H, Shahar M, Arpaia E, Lapidot Z, Leeder JS, Freedman M, Cohen A, Gazit A, Levitzki A and Roifman CM (1996) Inhibition of acute lymphoblastic leukaemia by a Jak-2 inhibitor. *Nature* **379**: 645-648.

Narain Y, Yip A, Murphy T, Brayne C, Easton D, Evans J.G, Xuereb J, Cairns N, Esiri MM, Furlong RA and Rubinsztein DC (2000) The ACE gene and Alzheimer's disease

susceptibility. *J.Med.Genet.* **37**: 695-697.

Negoro S, Kunisada K, Tone E, Funamoto M, Oh H, Kishimoto T and Yamauchi-Takihara K (2000) Activation of JAK/STAT pathway transduces cytoprotective signal in rat acute myocardial infarction. *Cardiovasc.Res.* **47**: 797-805.

Newhouse PA, Potter A, Kelton M, and Corwin J (2001) Nicotinic treatment of Alzheimer's disease. *Biol Psychiatry* **49**: 268-278.

Nordberg A, Hellstrom-Lindahl E, Lee M, Johnson M, Mousavi M, Hall R, Perry E, Bednar I and Court J (2002) Chronic nicotine treatment reduces beta-amyloidosis in the brain of a mouse model of Alzheimer's disease (APPsw). *J Neurochem* **81**: 655-658

Papke RL and Papke JKP (2002) Comparative pharmacology of rat and human α7 nAChR conducted with net charge analysis. *British Journal of Pharmacology* **137**(1)**:**49-61.

Romano C and Goldstein A. Stereospecific nicotine receptors on rat brain membranes. Science, *210*: 647-650, 1980.

Savaskan E, Hock C, Olivieri G, Bruttel S, Rosenberg C, Hulette C and Muller-Spahn F. (2001). Cortical alterations of angiotensin converting enzyme, angiotensin II and AT1 receptor in Alzheimer's dementia. *Neurobiol Aging* **22**: 541-546.

Seo J, Kim S, Kim H, Park C. H, Jeong S, Lee J, Choi S. H, Chang K, Rah J, Koo J, Kim E and Suh Y (2001) Effects of nicotine on APP secretion and A. *Biol Psychiatry* **49**: 240-247.

Sharlow ER, Pacifici R, Crouse J, Batac J, Todokoro K and Wojchowski DM (1997) Hematopoietic cell phosphatase negatively regulates erythropoietin- induced hemoglobinization in erythroleukemic SKT6 cells. *Blood* **90**: 2175-2187.

Shaw S, Bencherif M and Marrero MB (2002) Janus kinase 2, an early target of alpha 7 nicotinic acetylcholine receptor-mediated neuroprotection against Abeta-(1-42) amyloid. *J Biol Chem*

277: 44920-44924.

Wang H. Y, Lee DH, D'Andrea M.R, Peterson PA, Shank RP and Reitz AB (2000) beta-Amyloid(1-42) binds to alpha7 nicotinic acetylcholine receptor with high affinity. Implications for Alzheimer's disease pathology. *J.Biol.Chem.* **275**: 5626-5632.

Wang H, Yu M, Ochani M, Amella C. A, Tanovic M, Susarla S, Li J. H, Wang H, Yang H, Ulloa L, Al-Abed Y, Czura C.J and Tracey KJ (2003). Nicotinic acetylchone receptor α7 subunits is an essential regulator of inflammation**.** *Nature* **421**: 384-388.

JPET Fast Forward. Published on January 13, 2004 as DOI: 10.1124/jpet.103.061655
This article has not been copyedited and formatted. The final version may differ from this version.

FIGURE LEGENDS

Figure 1. Synthetic scheme for TC-1698

Figure 2. **The effects of TC-1698 on nAChR.** Responses of oocytes expressing human α4β2 receptors (A), human α7 receptors oocytes (B), human α3β2 (C), mouse muscle-type receptors α1β1εδ (D), or human α3β4 (E). Representative raw data traces are shown on the left, and concentration-response curves to the application of either ACh or TC-1698 are shown on the right. In the concentration-response curves, each point is the mean response of at least three cells (±SEM). Each measurement was initially normalized to the ACh control response measured in the same cell. These values were subsequently scaled by the ratio of the ACh controls to the ACh maximum response.

Figure 3. ACh and TC-1698 co-application responses of α4β2 nAChR. A) The effect of co-application of 1 μM TC-1698 on the response inhibition of an oocyte expressing human α4β2 receptors. On the left is shown the response to 30 μM ACh alone. On the right is the response of the same oocyte to 30 μM ACh plus 1 μM TC-1698. B) Inhibition curve for the effect of increasing concentrations of TC-1698 on the responses of α4β2-expressing oocytes to the application of 30 μM ACh co-applied with TC-1698. Each point is the mean response of at least three cells (±SEM). Each measurement is expressed relative to the ACh control response measured in the same cell prior to the co-application of ACh and TC-01698. C) Peak responses to high concentrations of ACh are relatively unaffected by co-application of TC-1698. On the left is shown the response to 1 mM ACh alone. On the right is the response of the same oocyte to 1 mM ACh plus 1 μM TC-1698. D) The effect of 1 μM TC-1698 on the inhibition of

JPET Fast Forward. Published on January 13, 2004 as DOI: 10.1124/jpet.103.061655
This article has not been copyedited and formatted. The final version may differ from this version.

responses to varying concentrations of ACh co-applied to oocytes expressing human α4β2 receptors. Data are normalized to the responses of the same oocytes to ACh alone applied at the indicated concentrations. Each bar is the mean response of at least three cells (±SEM).

Figure 4. TC-1698-Induced activation of JAK2, Akt and PI-3 Kinase in PC12 cells in the presence or absence of AG-490. PC12 cells pre-incubated in the presence or absence of the JAK2 inhibitor AG-490 (10 μM) are stimulated with 10 μM TC-1698 for the time indicated. Cells are immunoblotted with phospho-specific and non-phosphospecific anti-JAK2 and anti-Akt antibodies or with anti-PI-3-Kinase antibody. The PI-3-Kinase immunoprecipitated proteins are then immunoblotted with anti-phosphotyrosine and anti-PI-3-Kinase antibodies. Results shown for each immunoblot is representative of three immunoblots.

Figure 5. A. Effects of Ang II pretreatment with or without Ang II receptor antagonists on the TC-1698 induced activation of JAK2 in PC12 cells. Cells pre-incubated with Ang II for 8 hours in the presence or absence of AT_1 antagonist (candesartan) or AT_2 antagonist (PD 123177) were stimulated with TC-1698 for the time indicated. Cells are immunoblotted with phospho-specific and non-phosphospecific anti-JAK2. Results shown for each immunoblot is representative of three immunoblots. **B**. Angiotensin II-Induced phosphorylation of SHP-1 in PC12 cells. PC12 cells were incubated for 24 hours in serum-free medium before exposure to Ang II (100 nM) for the times indicated. Cells were lysed, and SHP-1 was immunoprecipitated from lysates with 10 μg/mL of anti-SHP-1 monoclonal antibodies and immunoblotted with anti-phosphotyrosine antibody. Results shown for each immunoblot is representative of three immunoblots. **C.** Effects of α-bungarotoxin on TC-1698 stimulated Jak-2 phosphorylation. Cells pre-incubated with 0.1

μM α-bungarotoxin or vehicle followed by addition of 0.1 μM TC-1698 for the time indicated. Results shown for each immunoblot is representative of three immunoblots.

Figure 6. **A.** TC-1698-Induced activation of JAK2 in PC12 cells in the absence or presence of Vanadate. PC12 cells preincubated in the presence or absence of the tyrosine phosphatase vanadate were stimulated with TC-1698 for the time indicated. Cells were immunoblotted with phospho-specific and non-phospho-specific anti-JAK2. **B.** Time-dependent increase in SHP-1 activity in the absence or presence of vanadate. Results shown for each immunoblot is representative of three immunoblots.

Figure 7. **A.** Effects of SHP-1 sense and antisense oligonucleotides on SHP-1 expression in PC12 cells. PC12 cells were treated with SHP-1 sense and antisense oligonucleotides for the times indicated and lysed. SHP-1 was immunoprecipitated from the lysates with anti-SHP-1 antibody. Precipitated SHP-1 proteins were then immunoblotted with specific anti-SHP-1 antibody. Results shown for each immunoblot is representative of three immunoblots **B.** Effects of SHP-1 antisense on the TC-1698- Induced activation of JAK2 in PC12 cells. Cells preincubated in the presence or absence of SHP-1 antisense or sense oligonucleotides were stimulated with TC-1698 for the time indicated. Cells were immunoblotted with phospho-specific and non-phospho-specific anti-JAK2. Results shown for each immunoblot is representative of three immunoblots.

Figure 8. **Effects of SHP-1 antisense on TC-1698-induced protection against Aβ and Ang II-induced apoptosis.** PARP expression was measured from lysates of cells treated with Aβ-(1-

42) peptide and/or Ang II in the presence or absence of TC-1698 and/or SHP-1 antisense. Results shown for each immunoblot is representative of three immunoblots.

Figure 9. Effects of SHP-1 antisense on the angiotensin II-induced activation of caspase-3. PC12 cells were incubated for the duration shown with Ang II in the presence of either SHP-1 antisense or SHP-1 sense or vanadate. Caspase-3 activities are shown as the mean ± S.E. of six independent cultures.

Figure 10. Schematic of the Protein Tyrosine Phosphatase SHP-1 inhibition of the alpha7-Jak2 survival pathway.

JPET Fast Forward. Published on January 13, 2004 as DOI: 10.1124/jpet.103.061655
This article has not been copyedited and formatted. The final version may differ from this version.

Table I: Binding selectivity profile of TC-1698. Data are mean percent inhibition of control binding (or activity) for duplicate determinations. No data denotes less than 25 % change in binding at 10 μM of TC-1698. For all non-nicotinic receptors tested TC-1698 had an $IC_{50} > 1$ μM.

Binding site	Radioligand	Inhibition (% at 10 μM)
Acetylcholinesterase	Acethylthiocholine	–
Adenosine, non selective	[^{3}H]-NECA	–
Adrenergic α_1 (rat cortex)	[^{3}H]-MeOxy-Prazocin	–
Adrenergic α_2 (rat cortex)	[^{3}H]-RX-821002	–
Adrenergic β non-selective	[^{3}H]- DHA	–
Angiotensin AT_1 (Human)	[^{125}I]-(Sar1-Ile8) Angiotensin	–
Angiotensin AT_2	[^{125}I] Tyr4-Angiotensin II	–
Calcium Channel, Type L	[^{3}H]- Nitrendipine	–
Bradykinin, BK2	[^{3}H]-Bradikinin	–
Calcium Channel, Type N	[^{3}H]- Conotoxin GVIA	–
Cholecystokinin, CCK1 (CCKA)	[^{125}I] CCK-8	–
Cholecystokinin, CCK2 (CCKB)	[^{125}I] CCK-8	–
Choline Acetyltransferase	[^{14}C]-Acetyl Coenzyme	–
Glutamic Acid Decarboxylase	[^{14}C]-Glutamic Acid	–
Corticotropin Releasing Factor	[^{3}H]-Tyr0-oCRF	–
Dopamine D3 (rat recombinant)	[^{3}H]-Spiperone	–
Dopamine transporter	[^{3}H]-WIN 35,428	–
Endothelin ET-A (Human)	[^{125}I]-Endothelin1	–
Endothelin ET-B (Human)	[^{125}I]-Endothelin1	–
GABA (rat cortex)	[^{3}H]-GABA	–
Estrogen	[^{125}I] 3,17B-Estradiol, 16a	–
GABA-A, BDZ, alpha1, central	[^{3}H]-Flunitrazepam	–
GABA-B transporter (rat cortex)	[^{3}H]-CGP 5462A	–
Galanin, Non-Selective	[^{125}I] Galanin	–
Glycine (rat spinal cord)	[^{3}H]-Strychnine	–
Histamine H1 periph. (Guinea-pig lung)	[^{3}H]-Pyrilamine	–

JPET Fast Forward. Published on January 13, 2004 as DOI: 10.1124/jpet.103.061655
This article has not been copyedited and formatted. The final version may differ from this version.

Histamine H1	[^{3}H]-Pyrilamine	–
Histamine H2	[^{3}H]-Pyrilamine	39
Histamine H3	[^{3}H]-Pyrilamine	60
Leukotriene B4, LTB4	[^{3}H]-LTB4	–
Leukotriene D4, LTD4	[^{3}H]-LTD4	–
Melatonin ML1 (chicken brain)	[^{125}I] -Iodomelatonin	–
Monoamine Oxidase A, Peripheral	[^{14}C]-5HT	–
Monoamine Oxidase B, Peripheral	[^{14}C]phenylethylamine	–
Muscarinic, M1 (human recombinant)	[^{3}H]-QNB	–
Muscarinic, M2 (human recombinant)	[^{3}H]-QNB	46
Muscarinic, non-selective central	[^{3}H]-QNB	–
Muscarinic, non-slective, Peripheral	[^{3}H]-QNB	–
Neurokinin, NK1	[^{3}H]-SP	–
Neurokinin, NK2 (Human Recombinant)	[^{3}H]-NKA	–
Neurokinin, NK3 (NKB)	[^{3}H]-Eledoisin	–
Nicotinic (rat cortex)	[^{3}H]-Cytisine	104
Norepinephrine transporter (rat cortex)	[^{3}H]-Nisoxetine	–
NOS (neuronal-Binding)	[^{3}H]-NOARG	–
Opioids (rat cortex)	[^{3}H]-Naloxone	–
Oxytocin (rat uterus)	[^{3}H]-oxytocin	–
Platelet Activating Factor, PAF	Hexadecyl-[^{3}H]-acetyl-PAF	–
Potassium K_{ATP} channels (rat cortex)	[^{3}H] -Glibenclamide	–
Potassium K_{VI} channels (rat cortex)	[^{125}I]-Apamin	–
Potassium K_{VS} channels (rat cortex)	[^{125}I]-Charybdotoxin	–
Serotonin Transporter	[^{3}H]-Citalopram, N-methyl	–
Serotonin, non-selective	[^{125}I]-LSD	–
Sigma (rat cortex)	[^{3}H]-DTG	35
Sodium channels Site 2 (rat cortex)	[^{3}H]-Batrachotoxin	–
Testosterone (cytosolic)	[^{3}H]-Methyltrienolone	–
Thromboxane A2 (Human)	[^{3}H]-SQ 29,548	–
Thyrotropin Releasing Hormone, TRH	[^{3}H]-(3MeHis2)TRH	–
Vasoactive Intestinal Peptide	[^{125}I]-VIP	–
Vasopressin V_1 (Rat aortic A7r5 cells)	[^{3}H]-AVP	–

JPET Fast Forward. Published on January 13, 2004 as DOI: 10.1124/jpet.103.061655
This article has not been copyedited and formatted. The final version may differ from this version.

Table II: Activation parameters for TC-1698.

	I_{max}	n	EC_{50}
α4β2	<0.05	NA*	(.03 ACh I_{max}@ 100 μM)
α7	1.0	0.9	345 ± 110 nM
α3β2	≤0.06	NA*	(0.05-0.02 ACh I_{max} 30-300 μM)†
α1β1εδ	0.28	2.0	20 ± 1.3 μM
α3β4	<0.05	NA*	(.02 ACh I_{max}@ 1mM)

*NA, not available. That is, the responses were too low for the data to give a meaningful curve fit.

† Between 30 and 300 μM there were detectable responses that varied between 0.05 and 0.02 of the ACh maximum response. However, responses to 30 μM and 100 μM were not statistically different and responses to 300 μM were, if anything, less than the responses to 100 and 30 μM.

JPET Fast Forward. Published on January 13, 2004 as DOI: 10.1124/jpet.103.061655
This article has not been copyedited and formatted. The final version may differ from this version.

Synthetic Scheme

Figure 1

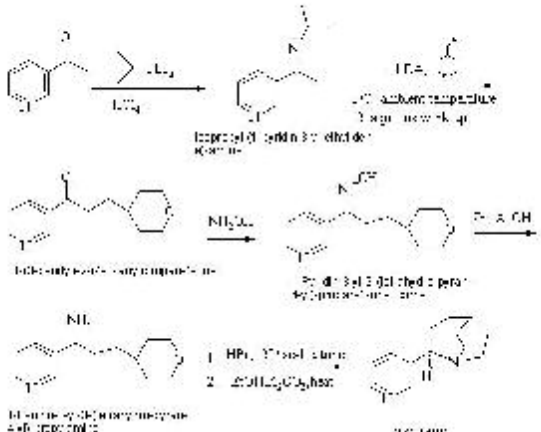

A

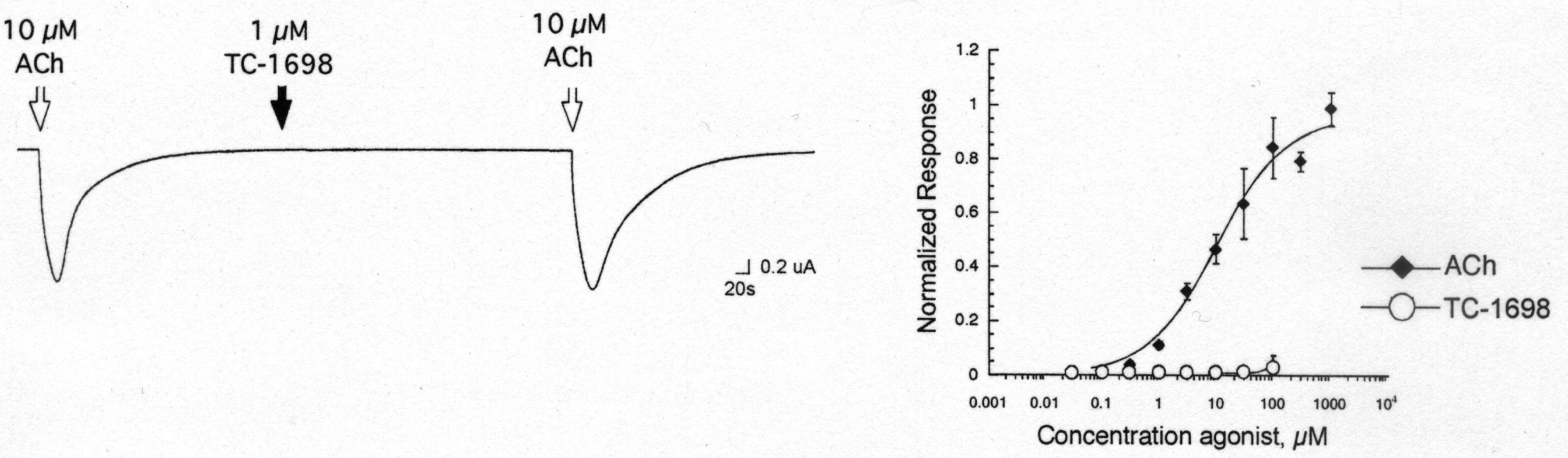

B

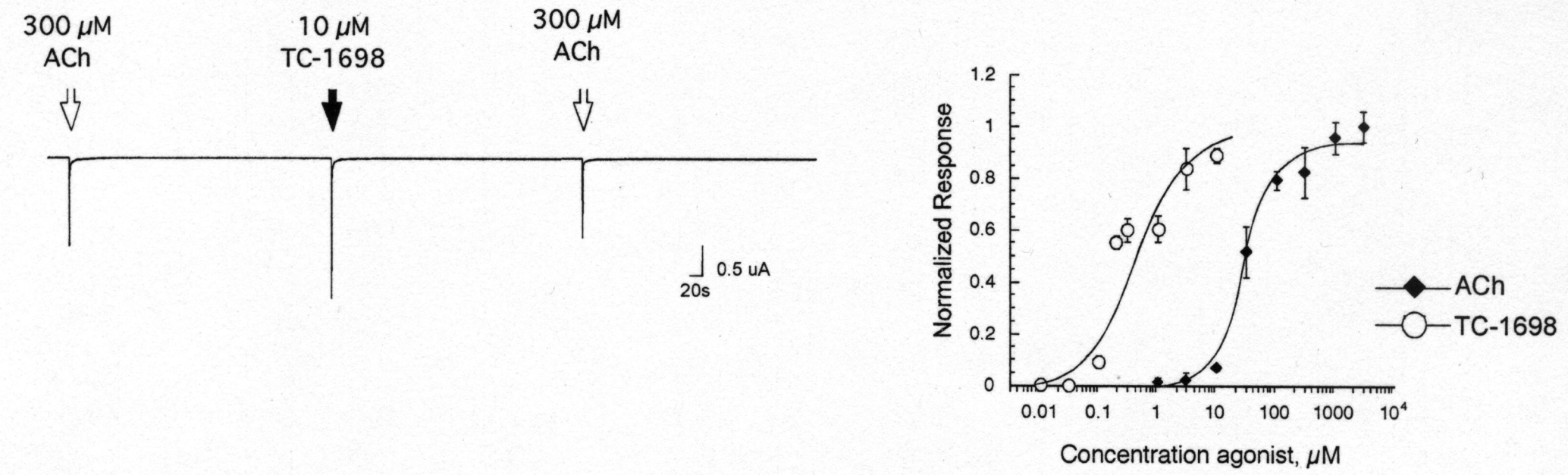

C

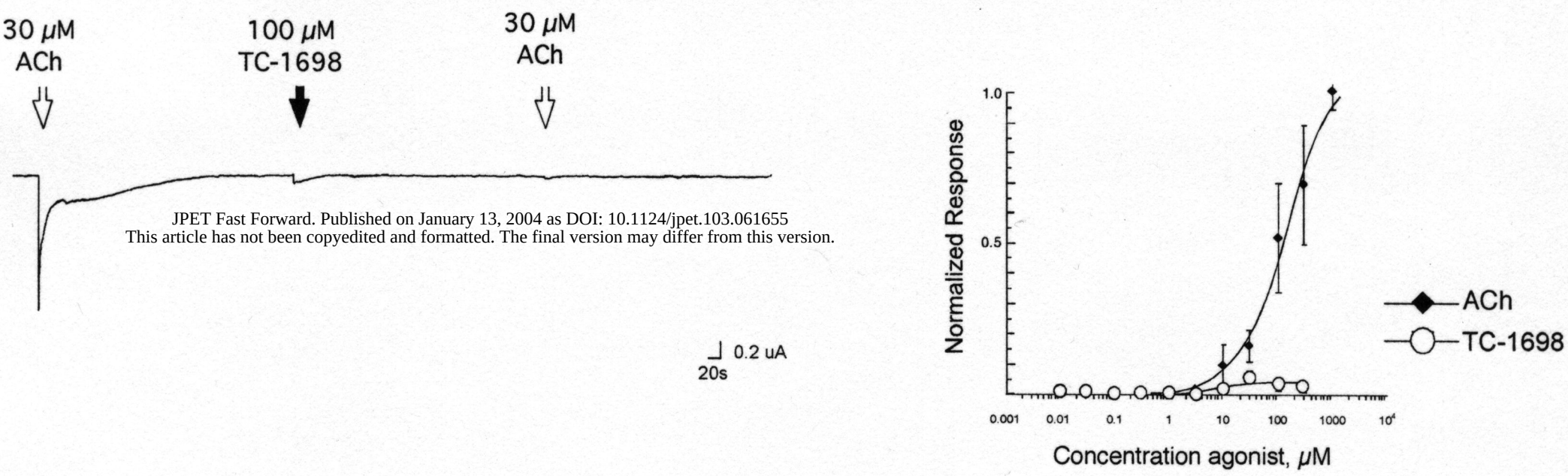

D

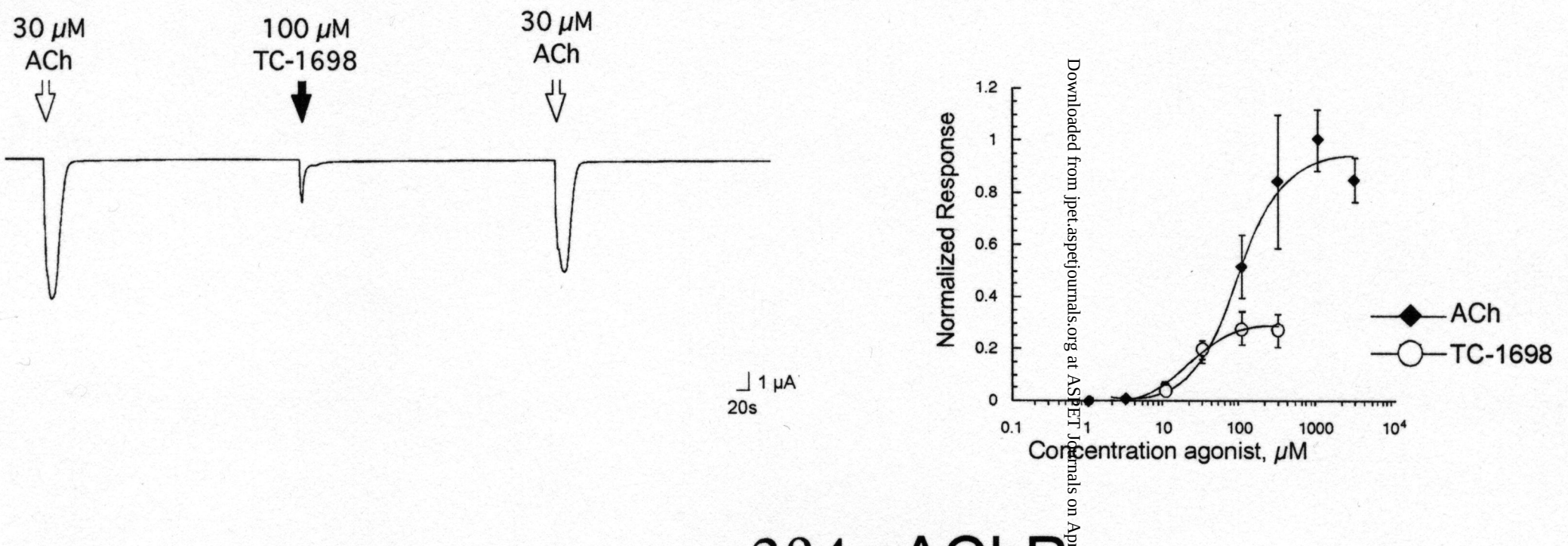

E

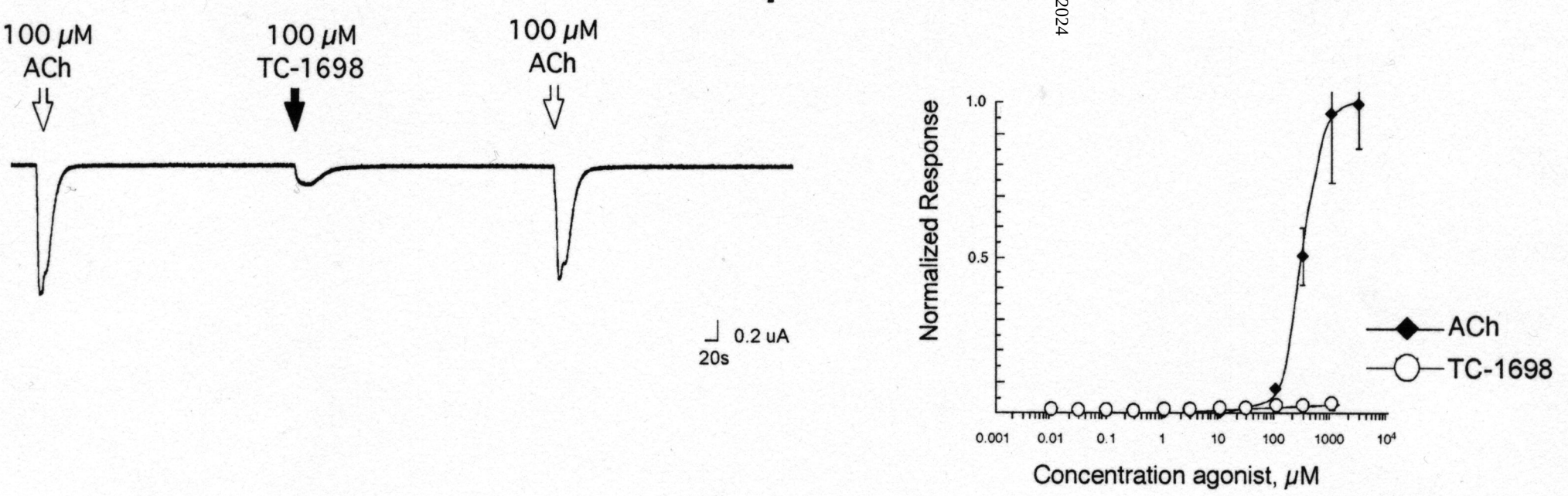

α4β2 nAChR

A

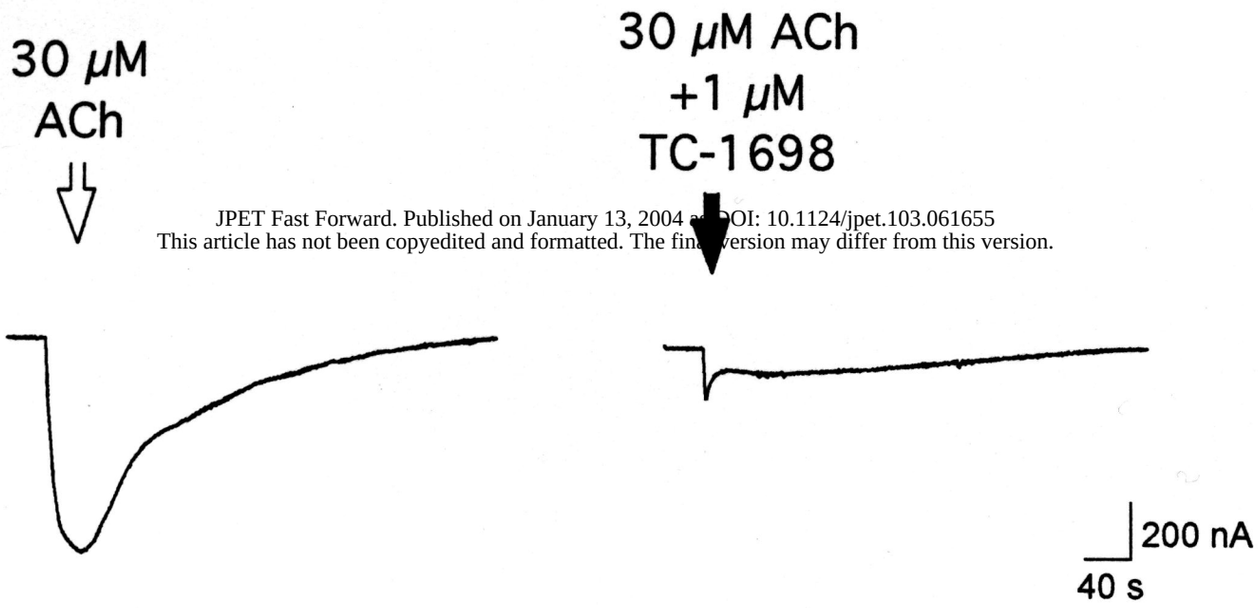

B

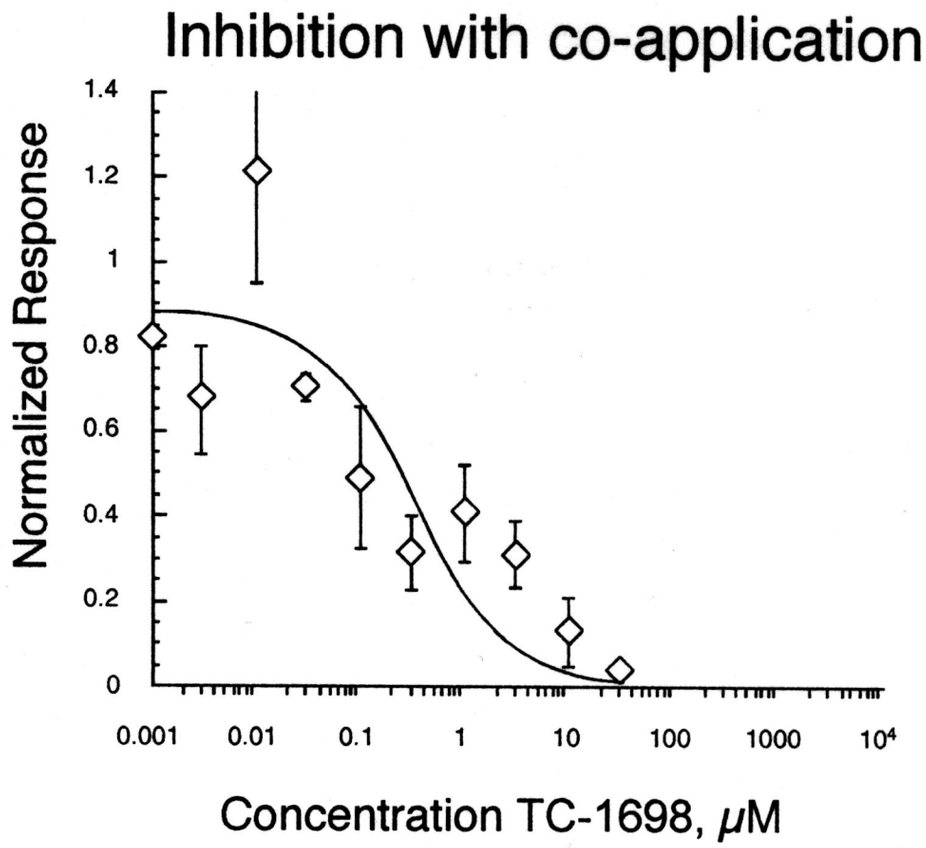

C

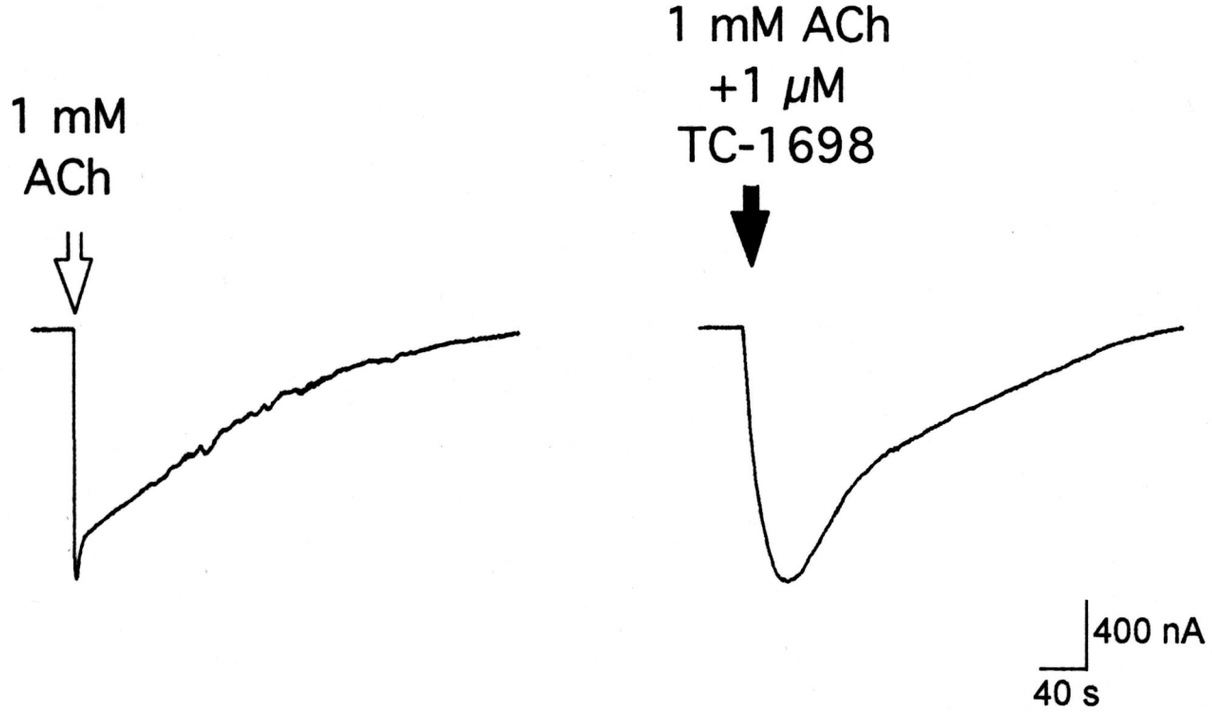

D

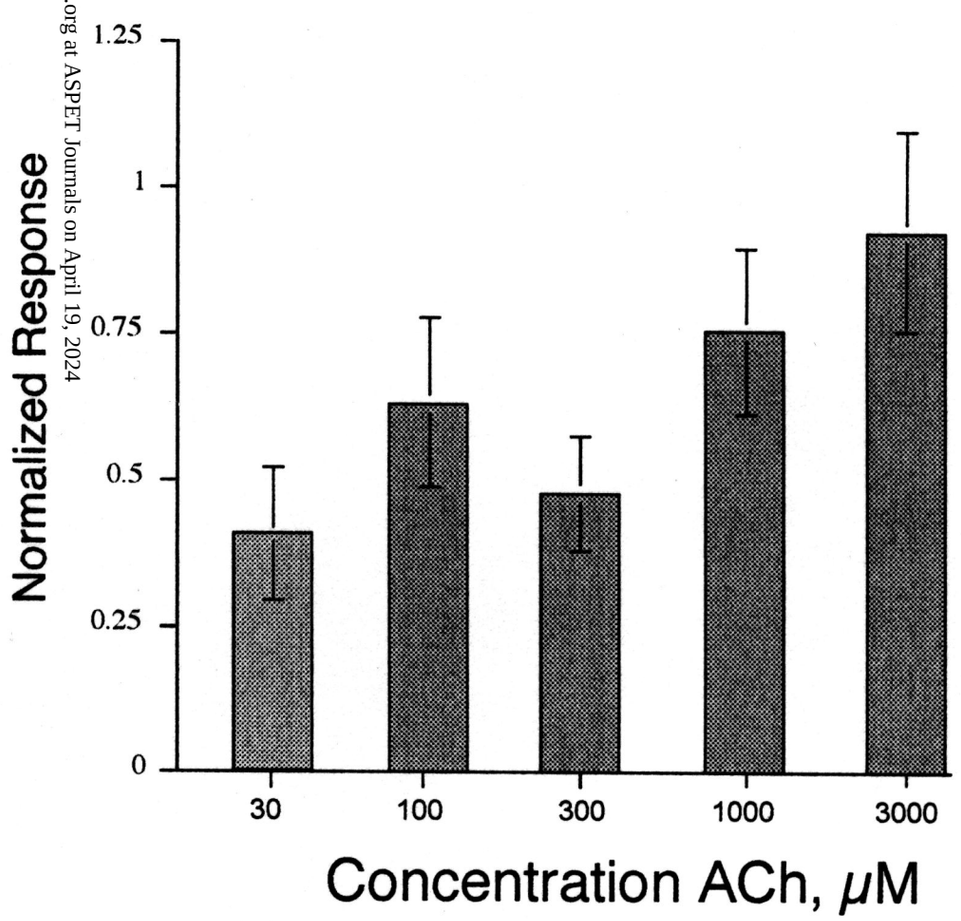

Figure 4

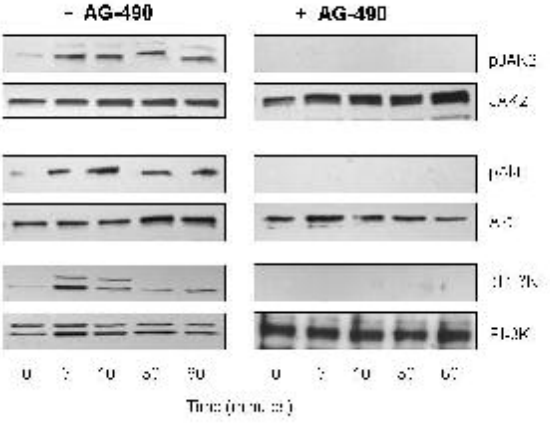
- AG-490
+ AG-490
pJAK2
JAK2
pSTAT
STAT
pERK
ERK
0
5
10
30
60
0
5
10
30
60

Figure 5

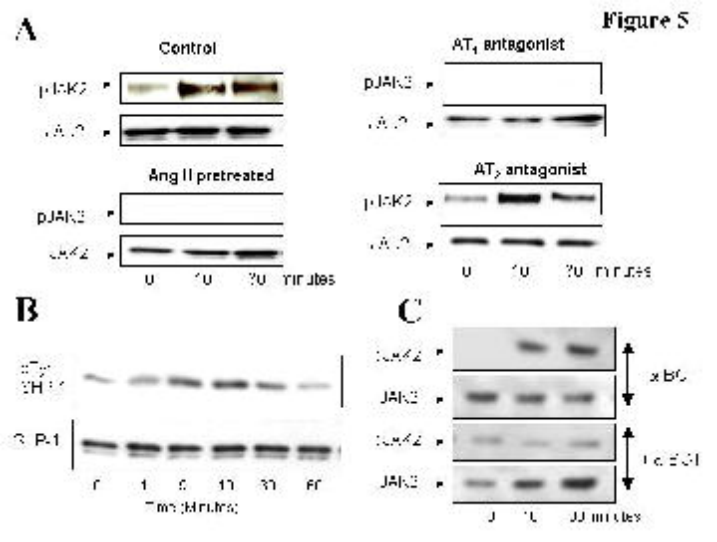
A
Control
pJAK2
JAK2
Ang II pretreated
pJAK2
JAK2
0
10
30 minutes
AT1 antagonist
pJAK2
JAK2
AT2 antagonist
pJAK2
JAK2
0
10
30 minutes
B
3 P-1
0
1
5
10
30
60
C
JAK2
JAK2
JAK2
JAK2
0
10
30 minutes

Figure 6

A

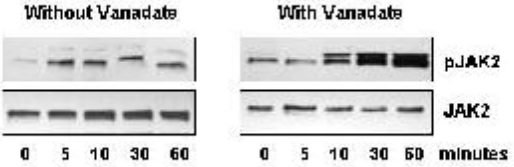
Without Vanadate
With Vanadate
pJAK2
JAK2
0 5 10 30 60
0 5 10 30 60 minutes

B

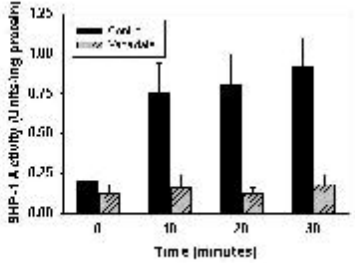
SHP-1 Activity (Units-ing protein)
1.25
1.00
0.75
0.50
0.25
0.00
0
10
20
30
Time (minutes)

Figure 7A

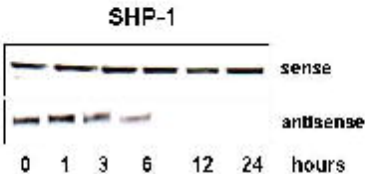

Figure 7B

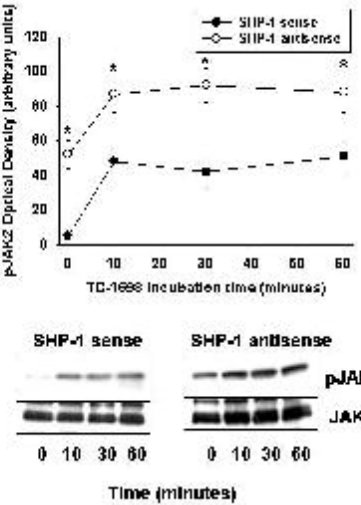
SHP-1 sense
SHP-1 antisense
pJAK2 Optical Density (arbitrary units)
120
100
80
60
40
20
0
0 10 20 30 40 50 60
TC-1666 incubation time (minutes)
SHP-1 sense
SHP-1 antisense
pJAK2
JAK2
0 10 30 60
0 10 30 60
Time (minutes)

Figure 8

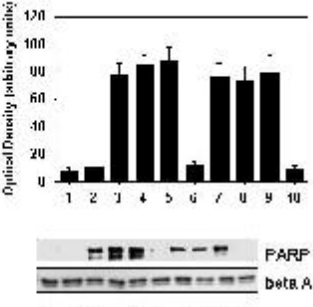

1. Control
2. TC-1698
3. ABeta (1-42)
4. AG-490
5. Angiotensin II
6. ABeta (1-42) + TC-1698
7. ABeta (1-42) + TC-1698 + AG-490
8. ABeta (1-42) + TC-1698 + Angiotensin II
9. ABeta (1-42) + TC-1698 + Angiotensin II + SHP-1 sense
10. Abeta (1-42) + TC-1698 + Angiotensin II + SHP-1 antisense

Figure 9

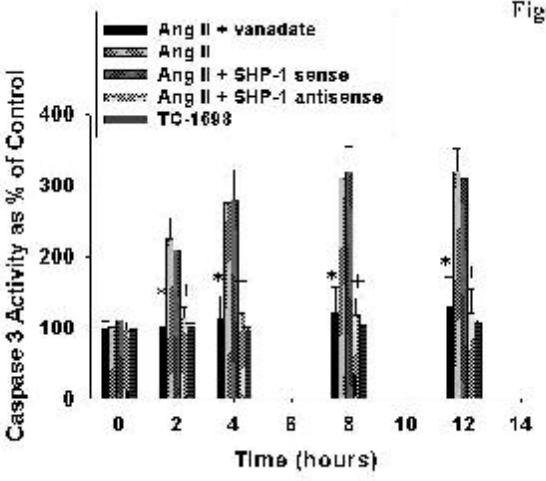
Ang II + vanadate
Ang II
Ang II + SHP-1 sense
Ang II + SHP-1 antisense
TC-1698
Caspase 3 Activity as % of Control
400
300
200
100
0
0
2
4
6
8
10
12
14
Time (hours)

Figure 10

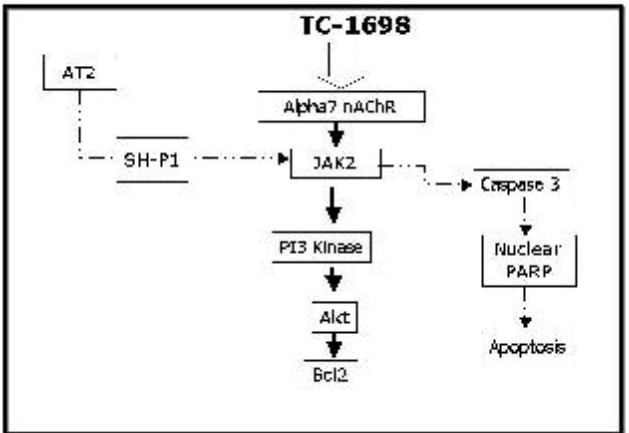
TC-1698
AT2
Alpha7 nAChR
SH-P1
JAK2
Caspase 3
PI3 Kinase
Nuclear PARP
Akt
Apoptosis
Bcl2